(v) Surprisingly, the Os(II) photosensitizers show much richer and more efficient photochemical behavior with $HgCl_2$ than similar Ru(II) photosensitizers. Thus, the Os(II) complexes may well prove to be better photosensitizers than the widely used Ru(II) systems.

(vi) Anionic NaLS micelles have proved useful in enhancing product separation by accelerating the expulsion of $HgCl_2^-$ before back-reaction with Os(III) can occur.

Acknowledgment. We gratefully acknowledge the donors of the Petroleum Research Fund, administered by the American Chemical Society, the Air Force Office of Scientific Research (Chemistry) (Grant AFOSR 78-3590), and the National Science Foundation (Grant CHE 82-06249). All lifetime measurements were performed on the University of Virginia laser facility, which was purchased in part with NSF Grant 77-09296. We thank W. Vining and T. J. Meyer for providing preprints.

Registry No. $HgCl_2$, 7487-94-7; NaLS, 151-21-3; terpy, 34795-04-5; phen, 73466-62-3; DPPM, 88841-74-1; DPPene, 88841-75-2; CNMe, 88841-76-3; COCl, 88853-97-8; water, 7732-18-5.

Contribution from the Department of Chemistry, University of Bern, CH-3000 Bern 9, Switzerland

Optical Spectra of Exchange-Coupled Manganese(II) Pairs in Cesium Magnesium Trichloride and Cesium Magnesium Tribromide

PAUL J. McCARTHY*[1] and HANS U. GÜDEL

Received August 4, 1983

Mixed crystals $CsMg_{1-x}Mn_xX_3$ (X = Cl, Br; x = 0.04–0.20) were prepared and investigated by optical spectroscopy. Manganese(II) pair excitations were observed in the regions of $^4A_1(G)$, $^4T_2(D)$, and $^4E(D)$ in the absorption spectra. They were studied as a function of temperature and applied magnetic field. Ground-state exchange parameters of 14.2 and 19.6 cm^{-1} were determined for $Mn_2Br_9^{5-}$ and $Mn_2Cl_9^{5-}$, respectively. The corresponding values for the singly excited $^4A_1$ pair state were found to be 18.6 and 26.8 cm^{-1}. Estimates of the orbital contributions to the net exchange were made.

Introduction

The study of pairs of paramagnetic transition-metal ions remains an active area of solid-state research. Ground-state properties are usually investigated by magnetochemical techniques. Valuable information about exchange splittings in the ground and excited states can, however, also be obtained from optical spectroscopy. This is particularly true for systems exhibiting sharp and structured spin-forbidden absorption or emission bands.

Reports have appeared on several systems related to those treated in this research. The optical spectra of the $^4A_1$ pair states of manganese(II) in $KMgF_3$ and $KZnF_3$ have been studied in detail.[2-6] Trutia et al.[7] have measured the optical spectra at 77 K of single crystals of $CdCl_2$ containing 15 and 0.1 mol % manganese(II). In the 15% crystals they observed bands not found in the 0.1% crystals, bands that had also been observed by Pappalardo[8] in pure $MnCl_2$. They noted that these bands do not belong to isolated $MnCl_6^{4-}$ groups. The spectra of $CsMnCl_3$ have been studied,[9] as well as those of some similar antiferromagnetic insulators: $RbMnCl_3$,[9] $TlMnCl_3$,[10] $((CH_3)_4N)MnCl_3$ (TMMC),[11] and Rb_2MnCl_4.[9,12] No report has appeared on the spectra of $CsMg_{1-x}Mn_xCl_3$.

The electronic spectra and magnetic properties of the one-dimensional antiferromagnet $CsMnBr_3$ and of the diluted analogue $CsMg_{1-x}Mn_xBr_3$ (x = 0.08, 0.26), between 77 and 300 K, have been reported by McPherson et al.[13] Since the spectra are only of low resolution, they show no traces of the pair effects reported here. A more detailed study of the optical spectrum of pure $CsMnBr_3$ has appeared,[14] as well as that of the analogous $((CH_3)_4N)MnBr_3$ (TMMB).[15]

In this research we have made a systematic study of the optical absorption spectra of the mixed crystals $CsMg_{1-x}Mn_xX$ (X = Br, Cl; $x \leq 0.2$) in the region of the spin-forbidden d–d transitions. Emphasis has been placed on features arising from $Mn_2X_9^{5-}$ pairs. The matrix used has some notable advantages: the crystal symmetry is high, and the symmetry of the $Mn_2X_9^{5-}$ pairs in the crystal is also high (D_{3h}). The threefold axis of the pairs coincides with the crystal c axis, and all dimers are parallel. This latter fact permits the measurement of the polarization of the pair bands, a unique advantage. It was not possible, for example, to do this for the manganese(II) pairs in $KMg_{1-x}Mn_xF_3$, which has the perovskite structure.[6]

Our aims in this research have been (1) to determine the energy splittings in the ground state and in as many excited pair states as possible, (2) to study the intensity mechanisms of the pair excitations, and (3) to attempt a rationalization of exchange splittings in terms of orbital parameters. From this, information can be obtained concerning the dominant exchange mechanism and exchange pathways, information not available from a magnetochemical study alone.

Experimental Section

Crystal Preparation. Crystals were prepared by the Bridgman technique. The bromide crystals contained 20, 14, 8, and 4 mol % manganese, while only a 5 mol % chloride sample was prepared. The

(1) To whom correspondence should be addressed at the Department of Chemistry, Canisius College, Buffalo, NY 14208.
(2) Ferguson, J.; Guggenheim, H. J.; Tanabe, Y. *J. Appl. Phys.* **1965**, *36*, 1046.
(3) Ferguson, J.; Guggenheim, H. J.; Tanabe, Y. *Phys. Rev. Lett.* **1965**, *14*, 737.
(4) Ferguson, J.; Guggenheim, H. J.; Tanabe, Y. *J. Phys. Soc. Jpn.* **1966**, *21*, 692.
(5) Ferguson, J.; Krausz, E. R.; Guggenheim, H. J. *Mol. Phys.* **1974**, *27*, 577.
(6) Ferguson, J.; Güdel, H. U.; Krausz, E. R.; Guggenheim, H. J. *Mol. Phys.* **1974**, *28*, 893.
(7) Trutia, A.; Ghiordanescu, V.; Voda, M. *Phys. Status Solidi B* **1975**, *70*, K19.
(8) Pappalardo, R. *J. Chem. Phys.* **1959**, *31*, 1050.
(9) Kambli, U. Doctoral Dissertation, University of Bern, 1983.
(10) Edelman, I. S.; Kotlyarskii, M. M.; Anistratov, A. T. *Phys. Status Solidi B* **1975**, *70*, K15.
(11) Day, P.; Dubicki, L. *J. Chem. Soc., Faraday Trans. 2* **1973**, *69*, 363.
(12) Popov, E. A.; Kotlyarskii, M. M. *Phys. Status Solidi B* **1979**, *96*, 163.
(13) McPherson, G. L.; Aldrich, H. S.; Chang, J. R. *J. Chem. Phys.* **1974**, *60*, 534.
(14) Cole, G. M.; Putnik, C. F.; Holt, S. L. *Inorg. Chem.* **1975**, *14*, 2219.
(15) Putnik, C. F.; Cole, G. M.; Holt, S. L. *Inorg. Chem.* **1976**, *15*, 2135.

0020-1669/84/1323-0880$01.50/0

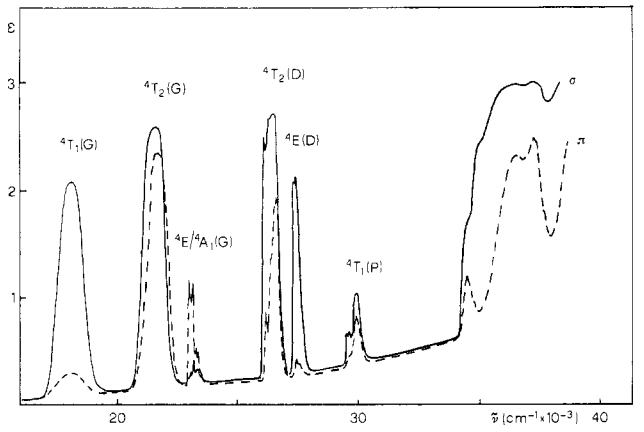

Figure 1. Single-crystal absorption spectra of $CsMnBr_3$ at 13 K. Octahedral labels are used although actual symmetry is trigonal.

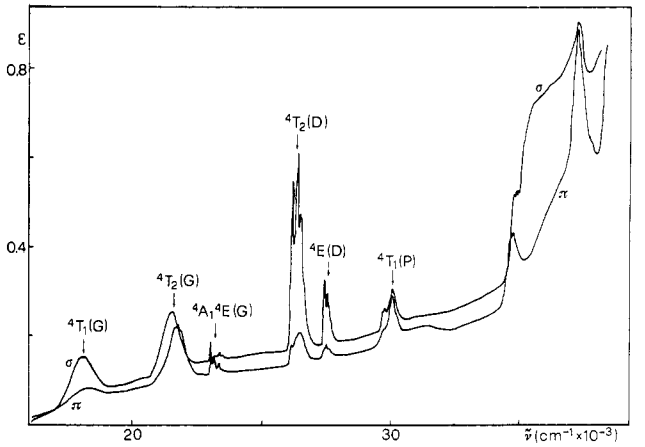

Figure 2. Same as Figure 1, but for $CsMg_{0.80}Mn_{0.20}Br_3$.

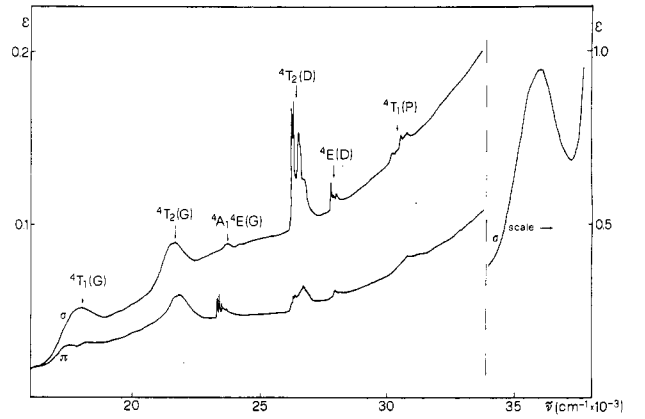

Figure 3. Same as Figure 1, but for $CsMg_{0.95}Mn_{0.05}Cl_3$.

compounds were characterized by their X-ray powder patterns.

When exact stoichiometric amounts were used in the preparation of $CsMg_{0.92}Mn_{0.08}Br_3$, the spectra showed several additional, highly structured bands (a large number of progressions in 158 cm^{-1}, the symmetric Mn–Br stretching frequency). These additional bands were shown to be due to tetrahedral $MnBr_4^{2-}$ (1) by their similarity to the bands of $((CH_3)_4N)_2MnBr_4$[16] and (2) by the fact that the crystal shows two luminescence maxima that match closely those reported for $((CH_3)_3NH)_3Mn_2Cl_7$,[17,18] which contains both linear chains of face-sharing $MnCl_6$ octahedra and discrete $MnCl_4^{2-}$ tetrahedra.[19] A second boule made with a small excess of $MgBr_2$ showed no tetrahedral manganese(II) bands.

Crystal Structures. $CsMgCl_3$ has been shown to belong to space group $P6_3/mmc$.[20] Isomorphous with this are the compounds $CsMgBr_3$,[21] $CsMgI_3$,[21] $CsMnBr_3$,[22] and $CsMnI_3$.[23] Although $CsMnCl_3$ belongs to space group $R\bar{3}m$[24] and so is not isomorphous with $CsMgCl_3$, a mixed crystal containing about 5 mol % manganese is not severely distorted from the structure of the host lattice. This is clear from the X-ray powder pattern. The former structures contain infinite linear chains of face-sharing octahedra, each consisting of a divalent metal ion surrounded by six halide ions. The cesium ions lie between the chains. An isolated MnX_6^{4-} group in the above lattices has point symmetry D_{3d}. When it is part of a pair, this same group has symmetry C_{3v}. The pair, $Mn_2X_9^{5-}$, belongs to point group D_{3h}.

The MgX_6 octahedron is slightly elongated along the trigonal axis in $CsMgX_3$ (X = Br, Cl).[21] Zero-field splittings in the ground state of $CsMg_{1-x}Mn_xCl_3$ have been determined by EPR spectroscopy.[20] They are of the order of 0.1 cm^{-1} and can be neglected in our optical study.

Spectroscopic Measurements. Some absorption spectra were obtained on a Cary-17 spectrophotometer equipped with an Air Products closed-cycle cryogenic refrigerator. With this apparatus, spectra were recorded down to 12 K. A pair of Glan–Taylor prisms were used to obtain plane-polarized light.

High-resolution spectra were made by dispersing the light of a halogen lamp or a sealed-beam xenon arc lamp (Varian) with a $^3/_4$-m monochromator (Spex 1702). Samples were cooled either by means of the helium flow-tube technique (lowest temperature about 6 K) or in an Oxford Instruments SM4 cryomagnet. With the latter, temperatures down to 1.4 K and magnetic fields up to 5 T were attained. Detection was made with a cooled photomultiplier tube (RCA 31034) using a chopper and a lock-in amplifier (PAR 186A). All energy values have been corrected to vacuum.

Results

Overall Spectra. The overall spectra of $CsMnBr_3$, $CsMg_{0.80}Mn_{0.20}Br_3$, and $CsMg_{0.95}Mn_{0.05}Cl_3$ are shown in Figures 1–3. (No spectrum for pure $CsMnCl_3$ is given, since it has a different space group.) In the figures, labels for octahedral symmetry are used for convenience, even though the actual symmetry is lower, due to the trigonal distortion along the c axis. σ and π in the figures refer to spectra recorded with the electric vector of light perpendicular and parallel to the c axis, respectively.

Assignment of the principal bands up to $^4T_1(P)$ is straightforward from a comparison with other manganese(II) d–d spectra and crystal field calculations.[25,26]

In general, the spectra show greatly enhanced intensity over those of crystals containing isolated manganese(II) complexes. This is due to an exchange intensity mechanism resulting from interactions between the metal centers and has been treated extensively.[26] This exchange-induced intensity has predominant polarizations for the various transitions. It is responsible for the pronounced dichroic ratios observed in the spectra of both the pure and diluted materials: σ dominance in $^4T_1(G)$, $^4T_2(D)$, and $^4E(D)$ and π dominance in $^4A_1(G)$.[11]

One spectrum (probably axial) of the very hygroscopic $CsMg_{0.92}Mn_{0.08}I_3$ was recorded at 12 K. Under conditions of moderate resolution no sharp bands characteristic of pair spectra were observed. The overall spectrum resembles in general detail those of the chloro and bromo complexes, but the principal bands lie about 500–1000 cm^{-1} lower in energy

(16) Vala, M. T.; Ballhausen, C. J.; Dingle, R.; Holt, S. L. *Mol. Phys.* **1972**, *23*, 217.
(17) Hardy, G. E.; Zink, J. I. *Inorg. Chem.* **1976**, *15*, 3061.
(18) Zink, J. I.; Hardy, G. E.; Gliemann, G. *Inorg. Chem.* **1980**, *19*, 488.
(19) Caputo, R. E.; Roberts, S.; Willett, R. D.; Gerstein, B. C. *Inorg. Chem.* **1976**, *15*, 820.
(20) McPherson, G. L.; Kistenmacher, T. J.; Stucky, G. D. *J. Chem. Phys.* **1970**, *52*, 815.
(21) McPherson, G. L.; McPherson, A. M.; Atwood, J. L. *J. Phys. Chem. Solids* **1980**, *41*, 495.
(22) Goodyear, J.; Kennedy, D. J. *Acta Crystallogr.* **1972**, *B28*, 1640.
(23) McPherson, G. L.; Sindel, L. J.; Quarls, H. F.; Frederick, C. B.; Doumit, C. J. *Inorg. Chem.* **1975**, *14*, 1831.
(24) Ting-I Li; Stucky, G. D.; McPherson, G. L. *Acta Crystallogr., Sect. B* **1973**, *B29*, 1330. Longo, J. M.; Kafalas, J. A. *J. Solid State Chem.* **1969**, *1*, 103.
(25) Hush, N. S.; Hobbs, R. J. M. *Prog. Inorg. Chem.* **1968**, *10*, 259.
(26) Ferguson, J. *Prog. Inorg. Chem.* **1970**, *12*, 159.

Table I. Energies (cm^{-1}) of Bands Containing Pair Transitions in $CsMg_{1-x}Mn_xX_3$

	X = Br[a]			X = Cl[b]	
state	band[c]	energy		band[c]	energy
$^4A_1$ (Figure 4)	1	22941.6	(Figure 5)	1	23353.0
	2A	51.6		2A	75.1
	3 (σ only)	58.2		3 (σ only)	80.6
	4B	60.4		4B	89.6
	5C	72.6		5C	23408.7
	6D	86.2		6	33.1
	7	97.6			
$^4T_2$ (Figures 7 and 8)	1B	26026	(Figure 9)	1B	26207.9
	2B	37.5		2B	27.6
	3B	48.8		3B	41.8
	4B	60.2		4A	61.7
	5A	67.6		5A	75.4
	6A	76.6		6A	92.8
	7 (π only)	82.1		7A	26315.8
	8A	90.6		8	27.4
	9A	98.6		9	35.4
	10	26106.6		10	48.2
	11	14.6		11	57.3
	12	22.3			
	13	30.3			
^4E (Figure 10)	1A	27309.1		1A	27794
	2A	14.6		2	27815
	3	23.4		3	37
	4	28.6		4	49 (sh)
	5	37.8			
	6	46.4			

[a] For the $^4A_1$ state, see Figure 4; for $^4T_2$, Figures 7 and 8; for ^4E, Figure 10. [b] For the $^4A_1$ state, see Figure 5; for $^4T_2$, Figure 9. [c] A–D refer to pair transitions originating in ground-state levels with $S = 1$–4, respectively.

than the corresponding bands in $CsMg_{0.80}Mn_{0.20}Br_3$. No further work was done on this system.

The spectra of the pure and doped bromide compounds (Figures 1 and 2) are quite similar in general appearance but differ considerably in the fine structure observed in several of the bands. This is a reflection of the different nature of the exchange effects in the two systems. In the doped crystals, we observe for most bands an increase in molar extinction coefficient as the concentration of manganese increases. The bands that involve pair transitions will be discussed in detail below. Concerning the remaining bands in the doped crystals, a few features are worth noting:

(1) The $^4T_2(G)$ absorption in π shows a short progression in 136 ± 3 cm^{-1}. The ground-state a_1 vibration is 161.5 cm^{-1}.[27] This lowering to 84% of the ground-state value is consistent with the fact that this transition involves an electron transfer between e and t_2 orbital sets and so results in a change in bonding parameters. The difference of 200 cm^{-1} in band position in the two polarizations may reflect the trigonal splitting of this $^4T_2$ level.

(2) The weak, broad absorption around 31 000 cm^{-1} (π) is absent from the spectra of the pure compound. Its relative intensity grows with *de*creasing manganese concentration. Its origin is uncertain.

(3) The band at 34 500 cm^{-1} is most likely the $^4A_2$ transition.[14] The intense absorption following this band consists of a strong shoulder (36 300 cm^{-1}) largely σ polarized and a strong peak at 37 200 cm^{-1}. The former can be assigned to the double excitation, $^6A_1{}^6A_1 \rightarrow {}^4T_1{}^4T_1$, which is expected to lie at approximately 36 560 cm^{-1}, twice the energy of the $^4T_1$ single excitation. The band is expected to be σ polarized, if spin–orbit coupling is neglected. Similar double-excitation bands were found in the spectra of $KMg_{1-x}Mn_xF_3$[6] and manganese(II)-doped NaF.[28] The band at 37 200 cm^{-1} is probably best assigned to the $^4T_1(F)$ state.

(4) In crystals containing 4 mol % manganese, bands are also seen at 39 400, 41 000, and 42 500 cm^{-1}. One of these may be a transition to the highest energy quartet state, $^4T_2(F)$, and the others are likely to be double excitations.

The lowest energy band in $CsMg_{0.95}Mn_{0.05}Cl_3$, $^4T_1(G)$, shows in π polarization two components separated by about 900 cm^{-1}, as did the analogous band in pure $CsMnCl_3$.[9] It appears to be a reflection of the trigonal distortion in the $MnCl_6$ group. The $^4T_2(G)$ band in π shows a short progression (three members clearly seen) in about 250 cm^{-1}. This is probably the completely symmetrical Mn–Cl stretching frequency, which in the ground state of $((CH_3)_4N)MnCl_3$ is at 256 cm^{-1}.[29] The strong band at 36 000 cm^{-1} appears to be completely σ polarized. It has, within experimental error, exactly twice the energy of the first band in the spectrum and it can be assigned to the double excitation, $^6A_1{}^6A_1 \rightarrow {}^4T_1{}^4T_1$.

$^4A_1{}^4E$ Region. Figure 4 shows a small part of the π spectrum of $CsMg_{0.80}Mn_{0.20}Br_3$. Bands A–D are predominantly π polarized, and their intensity is very temperature dependent between 4 and 40 K. None of these lines suffers any splitting upon the application of a magnetic field of 5 T $\perp c$. The energies of the bands are listed in Table I. The energy differences between bands A–B, B–C, and C–D are in a ratio of 1.0 to 1.4 to 1.6. The assignment of these bands to the $^4A_1$ pair transitions will be discussed below.

Band 1 is the lowest energy band in this region. It is extremely broadened in a magnetic field of 5 T $\perp c$, so much so that it virtually disappears. The weak, σ-polarized band 3 is also strongly affected by a magnetic field. It is possible that both absorptions are associated with the $^6A_1 \rightarrow {}^4E$ transition, which has been found to lie below $^6A_1 \rightarrow {}^4A_1$ in $KMg_{1-x}Mn_xF_3$.[30]

The prominent band 7 shows no clear-cut change in intensity with increasing temperature, nor is it split by a magnetic field of 5 T $\perp c$. From this and its concentration dependence it

(27) Breitling, W.; Lehmann, W.; Srinavasan, T. P.; Weber, R. *Solid State Commun.* **1976**, *20*, 525.
(28) Srivastava, J. P. *J. Phys. Chem. Solids* **1975**, *36*, 727.
(29) Adams, D. M.; Smardzewski, R. R. *Inorg. Chem.* **1971**, *10*, 1127.
(30) Ferguson, J.; Güdel, H. U.; Krausz, E. R.; Guggenheim, H. J. *Mol. Phys.* **1974**, *28*, 879.

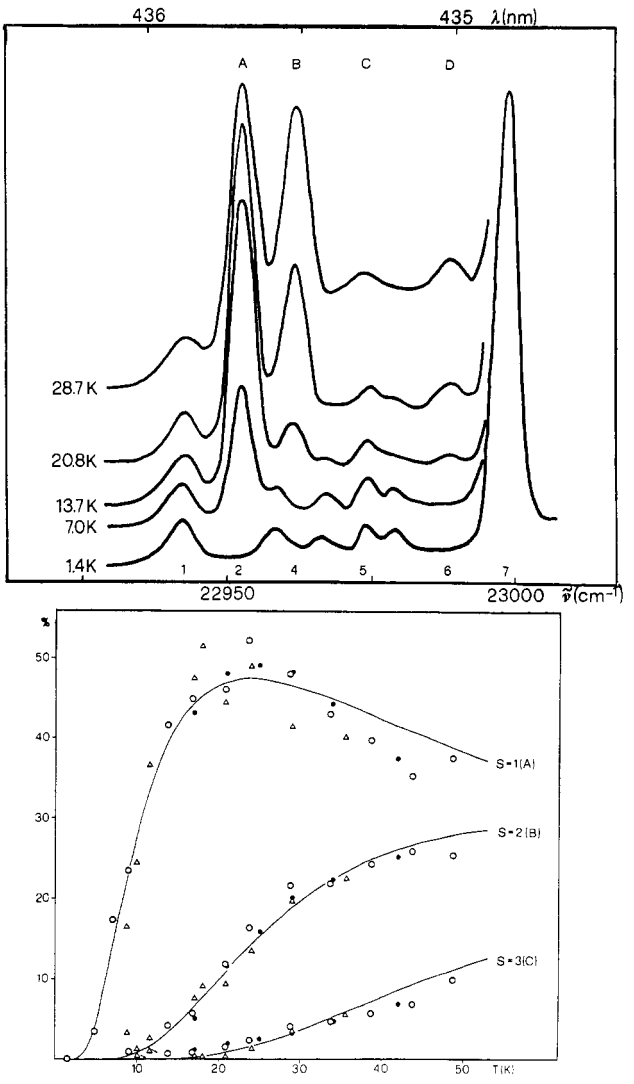

Figure 4. Top: Manganese(II) pair and single-ion excitations (π) to $^4A_1(G)$ in $CsMg_{1-x}Mn_xBr_3$ ($x = 0.20$). Bottom: observed band areas for three different crystals (○, $x = 0.20$; △ and ●, $x = 0.08$) and Boltzmann populations calculated with $J_{gs} = 14.2$ cm^{-1}.

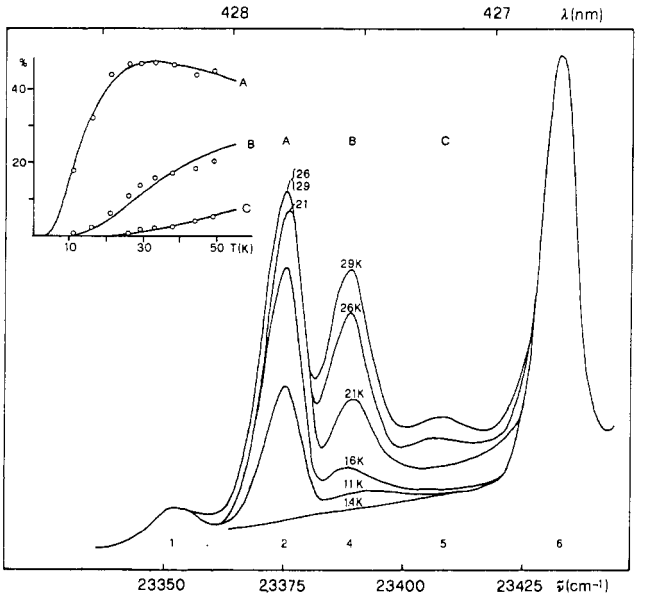

Figure 5. Same as Figure 4 (top), but for $CsMg_{0.95}Mn_{0.05}Cl_3$. Inset: observed band areas and Boltzmann populations calculated with $J_{gs} = 19.6$ cm^{-1}.

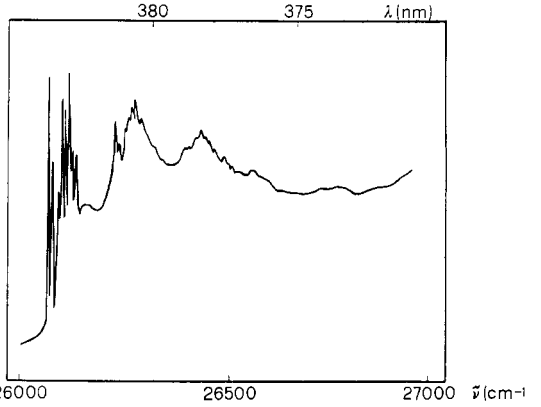

Figure 6. The $^6A_1 \rightarrow {}^4T_2(D)$ transitions (σ) of $CsMg_{0.92}Mn_{0.08}Br_3$ at 9.5 K.

can most probably be assigned to the single-ion $^6A_1 \rightarrow {}^4A_1$ transition.

An unresolved multiple band whose intensity strongly increases with increasing manganese concentration lies about 17 cm^{-1} above band 7. It is most likely due to triples.

The weak absorptions between 22 950 and 22 980 cm^{-1} shown in the 1.4 K spectrum in Figure 4 cannot be assigned with certainty. They are, however, either single-ion absorptions or due to triples or higher clusters. They will not be discussed further.

In the 20% sample there are a number of weak absorptions in π polarization between 23 020 and 23 325 cm^{-1}, which have not been investigated in detail. One noticeably temperature-sensitive band, however, lies 144 cm^{-1} above the first $^4A_1$ pair band. The band approaches zero intensity at 1.4 K but does not disappear entirely. So, it is probably a vibronic line associated with the pair spectra, but overlying some other very weak absorption. A similar band is seen in the chloride spectrum (π) 228 cm^{-1} above the first $^4A_1$ pair line.

Figure 5 shows the π spectrum of the $^4A_1$ pair region of $CsMg_{0.95}Mn_{0.05}Cl_3$, and the energies of all bands are listed in Table I. The bands shown are completely π polarized. The chloride spectrum in this region is quite similar to that of the bromide, and similar assignments can readily be made. Bands A–C are, however, more widely separated than in the bromide spectrum; the ratio of the separations A–B to B–C is 1.0 to 1.3. The temperature dependence also is less steep than in the case of the bromide. As will be seen, these results indicate that the chloride has greater exchange splittings in both ground and excited states. A pair of bands of moderate intensity lie 18.5 and 35.9 cm^{-1} above band 6; exact assignment is not at present possible.

$^4T_2(D)$ Region. In the bromide complex the σ spectrum of this band at 9.5 K shows an initial group of sharp bands, with the group being repeated with decreasing resolution about four more times (Figure 6). From the very sharp peaks in the first two sets at about 10 K, a separation of 158.6 ± 0.4 cm^{-1} is measured, corresponding to a progression in the Mn–Br symmetric stretching frequency. In the Raman spectrum at 2 K this is found at 161.5 cm^{-1}.[27] This near-identity of the ground-state and excited-state values is consistent with the fact that both states consist of terms from $t_2{}^3e^2$. The electron pairing in the t_2 set appears to cause little change in the character of the Mn–Br bond. The intensity distribution in the progression suggests, on the other hand, an increase of about 0.08 Å in the Mn–Br bond distance in the excited state.[31] A periodicity of about 150 cm^{-1} has been noted in this band in the spectrum of $MnBr_2$ but was not definitely assigned.[8]

Between 26 025 and 26 135 cm^{-1}, that is, within the first group of bands, at about 25 K there are 13 bands; see Figures

(31) Ballhausen, C. J. *Theor. Chim. Acta* **1962**, *1*, 285.

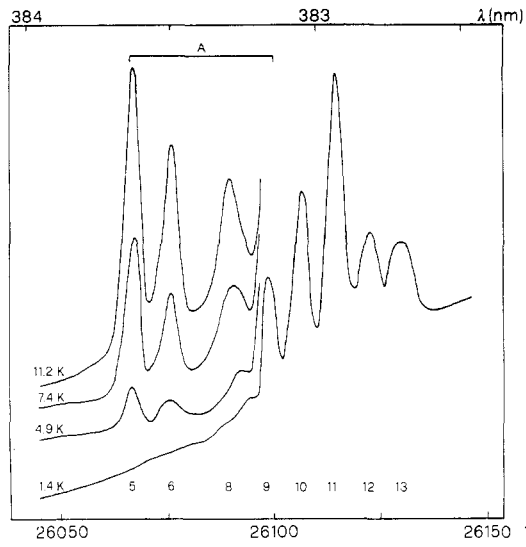

Figure 7. Manganese(II) pair and single-ion excitations (σ) to $^4T_2(D)$ in $CsMg_{0.92}Mn_{0.08}Br_3$.

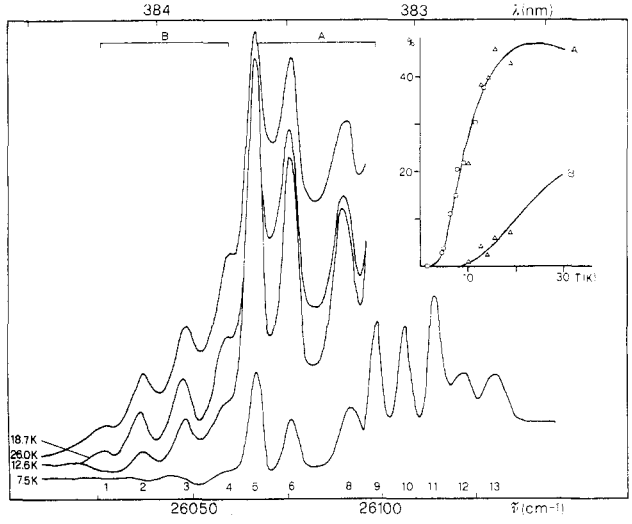

Figure 8. Same as Figure 7, but for a different temperature range. Inset: observed band areas for two different crystals and Boltzmann populations calculated with $J_{gs} = 14.2$ cm^{-1}.

7 and 8 and Table I. All appear in the σ spectrum except band 7, which is completely π polarized. Bands 5–13 are also seen in π, but with only about 30% the intensity found in σ. At 1.4 K bands 1–6 and 8 are completely absent. When the crystals are warmed to 5 K, bands 5, 6, 8, and 9 (A bands) increase rapidly in intensity. In the temperature range 2–8 K, bands 11 and 12 decrease about 15–20% and band 7 decreases about 35% in size. Between 8 and 13 K bands 11 and 12 show little further change. When they are further warmed, bands 1–4 (B bands) appear in σ. No attempt was made to monitor their presence in π because of their weakness and somewhat diffuse character. The band groups A and B that are completely absent at 1.4 K show the same temperature dependence as bands A and B in the $^4A_1$ region. The remaining bands probably represent single-ion transitions. Band 9 appears to be a single-ion transition overlying an A pair band. Bands 7, 11, and 12 will be discussed below.

In distinction to the situation with the $^4A_1$ pair lines, which are unchanged by a magnetic field of 5 T $\perp c$, all the lines in the $^4T_2$ region appear to be broadened or split by fields of 2 and 4 T $\perp c$.

The spectra of the chloride complex (Figure 9) show features similar to those found for the bromide complex. Two sets of bands, absent at 1.4 K, increase in intensity as the temperature

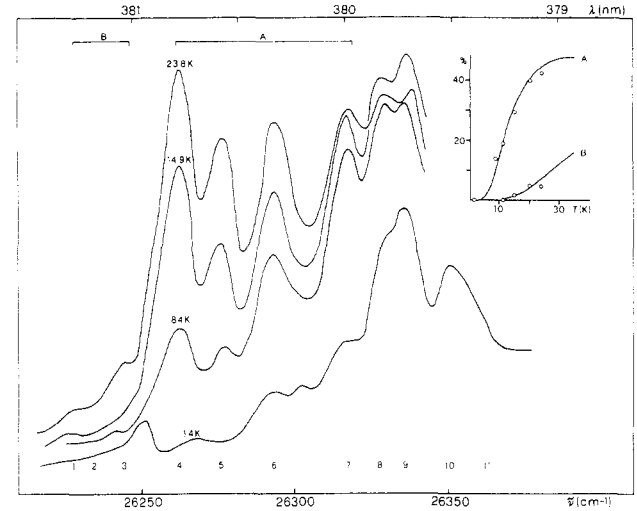

Figure 9. Same as Figure 7, but for $CsMg_{0.95}Mn_{0.05}Cl_3$. Inset: observed band areas and Boltzmann populations calculated with $J_{gs} = 19.6$ cm^{-1}.

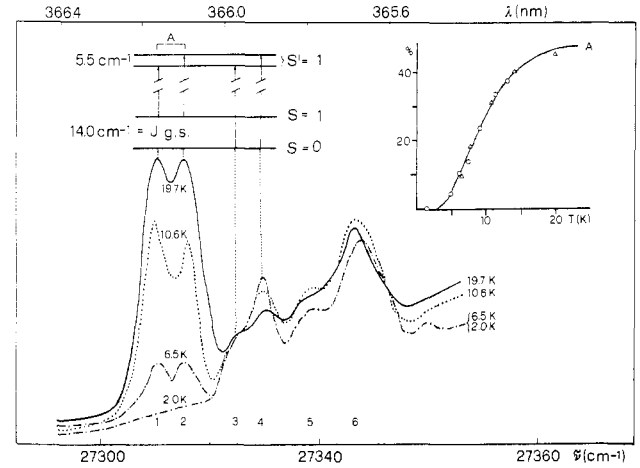

Figure 10. Manganese(II) pair and single-ion excitations (σ) to $^4E(D)$ in $CsMg_{0.92}Mn_{0.08}Br_3$. Inset: observed band areas and Boltzmann populations calculated with $J_{gs} = 14.2$ cm^{-1}.

is raised, bands A appearing first and then bands B. They are almost completely σ polarized and are assigned as in the bromide complex to pair transitions. Band energies are listed in Table I.

Built on the spectrum shown in Figure 9 is a poorly defined progression of about 240 cm^{-1}, the symmetric Mn–Cl stretching mode in the excited state. A precise value could not be determined, since no exact correlation between fine structure in the first and second broad bands could be made, as was done in the case of the bromide. The ground-state value for the a_1 mode of the matrix $CsMgCl_3$ at 2 K is 251.0 cm^{-1},[27] and the value from the Raman spectrum of TMMC at 120 K is 256 cm^{-1}.[29]

The π spectrum at 1.4 K shows some weak and poorly resolved features, not, however, at the positions of the principal bands in the σ spectrum. No analysis could be made.

$^4E(D)$ Region. In the spectra of the bromide complex, the $^4E(D)$ band is strongly σ polarized. The region of particular interest is shown in Figure 10, and the band positions are listed in Table I. Bands 1 and 2 are absent at 2 K and appear with increasing intensity as the temperature is raised. This hot-band behavior is the same as that observed for band A in the $^4A_1$ region, and the assignment of bands 1 and 2 to manganese pair transitions is therefore straightforward. A weak shoulder (not shown in the figure) is also observed on the low-energy side of band 1. Bands 3 and 4 decrease in size by about 50%

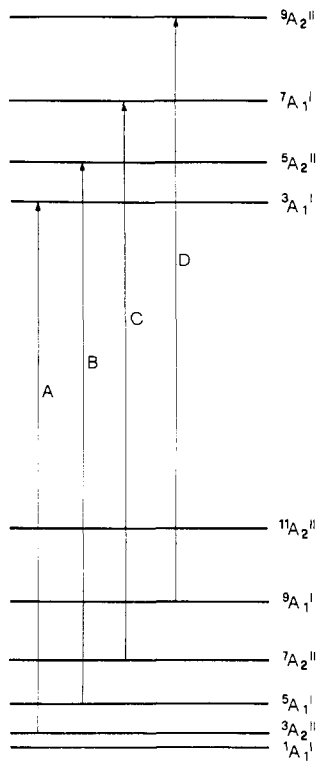

Figure 11. Single excitations to $^4A_1$ in $Mn_2X_9^{5-}$. The transitions are designated as in Figures 4 and 5.

between 2 and 20 K (see Figure 10). Bands 5 and 6 seem relatively insensitive to temperature in the range shown.

The bands in this region show changes on the application of a magnetic field. In particular, lines 1 and 2 show some splitting. This contrasts with the behavior of the $^4A_1$ pair lines, which are unaffected by a magnetic field.

The ^4E band system in the chloride complex is also strongly σ polarized. The positions of the bands observed in this region are listed in Table I, and their assignment is discussed below. Due to poor resolution of the spectra, no band areas could be measured and no figure is shown for this transition.

Discussion

Ground-State Exchange Splitting. Exchange interactions in the electronic ground state of a manganese(II) dimer are adequately described by a Heisenberg Hamiltonian

$$\hat{H}_{ex} = J_{gs}(\vec{S}_a \cdot \vec{S}_b) \tag{1}$$

where J_{gs} is the ground-state exchange parameter and $\vec{S}_a$ and $\vec{S}_b$ represent the total spins ($S_a = S_b = {}^5/_2$) on each of the two ions of the pair. The eigenvalues of eq 1 are readily obtained as

$$E(S) = J_{gs}/2[S(S+1) - {}^{35}/_2] \tag{2}$$

The energy splitting corresponds to a Landé pattern as shown for antiferromagnetic coupling in Figure 11. The energy separation between the singlet and triplet dimer levels is equal to J_{gs}. The pair wave functions are eigenfunctions of the total spin and transform as irreducible representations of D_{3h}.[11]

$^4A_1$ Singly Excited State. The $^4A_1$ single-ion state of manganese(II) derives from the same electron configuration $t_2^3e^2$ as the $^6A_1$ ground state. In this special situation in which both ions have the same configuration, namely half-filled 3d-electron shells, the exchange coupling can be treated by using a formalism proposed by Tanabe and co-workers.[4] The appropriate Hamiltonian is given by

$$\hat{H}_{ex}' = \sum_{ij} J_{ai\,bj}(\vec{s}_{ai} \cdot \vec{s}_{bj}) \tag{3}$$

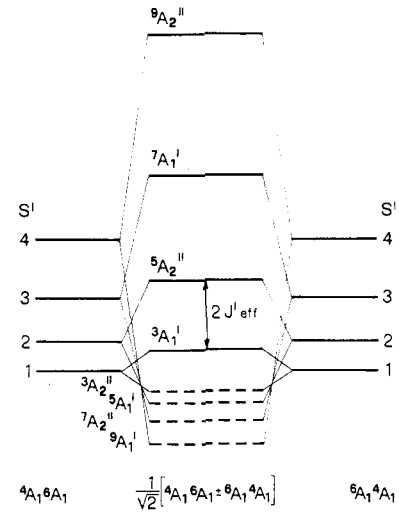

Figure 12. Exchange splitting of the singly excited $^4A_1$ pair state of $Mn_2X_9^{5-}$ (schematic).

where i and j number the trigonal orbitals t^0, t^+, t^-, e^+, and e^-. Singly excited pair states, in which the excitation is localized on ions a and b, respectively, can be represented by

$$|^4A_1{}^6A_1\rangle \quad \text{and} \quad |^6A_1{}^4A_1\rangle \tag{A}$$

The locally excited states (A) are eigenstates of the pair, only in the absence of any interaction between a and b. Their energies are degenerate and correspond to a single $^6A_1 \rightarrow {}^4A_1$ excitation. This is, however, not the situation in which we are interested. Under the action of (3), the states (A) are coupled and the proper pair wave functions have the form

$$\phi_\pm = (1/2^{1/2})[|^4A_1{}^6A_1\rangle \pm |^6A_1{}^4A_1\rangle] \tag{4}$$

The energy separation between ϕ_- and ϕ_+ is $2H_{ab}'$. The coupling element H_{ab}', which is also called a resonance or excitation-transfer matrix element, is given by

$$H_{ab}' = \langle {}^4A_1{}^6A_1|\hat{H}_{ex}'|{}^6A_1{}^4A_1\rangle \tag{5}$$

The energetic consequences of this are shown in Figure 12. The off-diagonal matrix elements H_{ab}' can be as large as, or larger than, the corresponding diagonal elements and thus play a dominant part in the energy splitting. Another consequence of the matrix elements in (5) is the delocalization of the excitation. It is equally shared between the two ions a and b, and the rate of excitation transfer between them can be estimated from time-dependent perturbation theory as[32]

$$f = (2H_{ab}')/\hbar \tag{6}$$

For the $^4A_1$ excitation in our manganese(II) pair, the order of magnitude of the H_{ab}' integral is 10–100 cm^{-1} and the corresponding transfer rate is 10^{12}–10^{13} s^{-1}.

Of the eight excited pair levels only the upper four in Figure 12 have the right symmetry to be spectroscopically accessible from the ground-state levels (see Figure 11).

A lengthy derivation using the formalism in ref 4 leads to the following expression for $J_{eff}'(^4A_1)$ in terms of the orbital parameters of (3):

$$J_{eff}'(^4A_1) = {}^1/_{25}[{}^{25}/_{18}\Sigma J_{tt} + {}^{25}/_{24}\Sigma J_{ee} + {}^{25}/_{18}\Sigma J_{te}] \tag{7}$$

The sums in (7) comprise all the orbital combinations; t and e stand for t^0, t^+, t^- and e^+, e^-, respectively. The corresponding expression for the ground-state exchange parameter is

$$J_{gs} = {}^1/_{25}[\Sigma J_{tt} + \Sigma J_{ee} + 2\Sigma J_{te}] \tag{8}$$

(32) Craig, D. P.; Walmsley, S. H. "Excitons in Molecular Crystals"; W. A. Benjamin: Amsterdam, 1968; p 6.

Within this theoretical framework we can assign the dimer bands in Figure 4 to the transitions A–D; this is illustrated in Figure 11. The selection rule is $A_1' \leftrightarrow A_2''(\pi)$. The $^4A_1$ pair transitions are expected to be π polarized and are found to be almost completely so. The different temperature dependences of the four bands reflect different Boltzmann factors for the $S = 1$–4 ground levels. All four bands correspond to $\Delta S = 0$ transitions, and no evidence of $\Delta S = \pm 1$ pair transitions is found in the spectra. This is a clear indication that their intensity is predominantly exchange induced. An exchange-induced intensity mechanism has also been found to be responsible for the analogous pair transitions in $KMg_{1-x}Mn_xF_3$.[6] It is also the cause of the relatively high extinction coefficients of the pure material, $CsMnBr_3$, in the visible range. Similar comments apply to the chloride complex (Figure 5).

If the exchange mechanism of Tanabe and co-workers[4] is assumed, the intensities of the bands will be in an A:B:C:D ratio of 7:30:63:75. The intensity ratios observed for the first three bands are 7:15:34 for the bromide and 7:20:61 for the chloride. The discrepancies between theory and experiment are not too drastic. They can be due to some intensity contributions from a single-ion mechanism and to the approximations inherent in the theory.

From the observed temperature dependences included in Figures 4 and 5 the ground-state splitting pattern is derived by a least-squares fit of the Boltzmann populations. The best agreement is obtained for J_{gs} values of 14.2 and 19.6 cm^{-1} for bromide and chloride, respectively. The value for the bromide is in excellent agreement with a value of 14.5 ± 0.5 cm^{-1} determined by inelastic neutron scattering on $CsMg_{0.86}Mn_{0.14}Br_3$.[33] In pure $CsMnBr_3$, J_{gs} values of 14.2 and 13.8 cm^{-1} were estimated from the magnon dispersion measured along c^* by inelastic neutron scattering[34] and magnetic susceptibility measurements,[35] respectively. The coupling is accordingly very similar in the dimer and the concentrated material, and next-nearest-neighbor interactions can to a good approximation be neglected in the one-dimensional antiferromagnet $CsMnBr_3$. The value of J_{gs} for the chloride (19.6 cm^{-1}) may be compared with the value obtained for TMMC from a plot of susceptibility vs. temperature, namely 18.2 cm^{-1}.[36]

From the ground-state splitting and the observed energy intervals between bands A–D it is possible to determine the excited-state splitting. If we assume a Landé-type splitting in the excited state, we can determine J_{eff}'. From the experimental energy separation between bands A and B, we find J_{eff}' values of 18.6 and 26.8 cm^{-1} for the bromide and chloride systems, respectively. The experimental energy intervals, 1.0:1.4:1.6 (Br) and 1.0:1.3 (Cl), deviate from the Landé pattern expected from our simple theory, namely 1.0:1.5:2.0. Deviations of the kind that we observe are expected if higher order terms contribute to the exchange. In the ground state these are biquadratic terms, and in the excited states they have a more complicated form.[37] While our data do not warrant a detailed analysis of these effects, the observed deviations from a Landé pattern clearly indicate their presence.

Using the experimental J_{gs} and J_{eff}' values together with (7) and (8), we can estimate the dominant orbital contributions to the total exchange. It is clear that an unambiguous determination of all the three sums in (7) and (8) is not possible on the basis of two experimental parameters. The following statements can, however, be made:

(1) If we assume the chemical bonding and thus the orbital parameters $J_{a_i b_j}$ are the same in the ground and excited state, $\sum J_{tt}$ must be the dominant antiferromagnetic term. A ratio J_{eff}'/J_{gs} of 1.39 is expected if $\sum J_{ee}$ and $\sum J_{te}$ do not contribute at all. The experimental ratios of 1.31 and 1.37 for the bromide and chloride, respectively, are close to this. Of the nine terms in $\sum J_{tt}$ we expect $J_{t^0t^0}$ to dominate all the others because the totally symmetric t^0 orbitals point directly toward each other.

(2) $\sum J_{ee}$ could be the leading antiferromagnetic term only if the orbital parameters $J_{a_i b_j}$ are about one-third larger in the excited state than in the ground state. Despite the fact that both the $^6A_1$ and the $^4A_1$ states derive from the same electron configuration, $t_2^3e^2$, this possibility cannot be excluded.

(3) $\sum J_{te}$ cannot be a dominant term. Its contribution is either negligible or weakly ferromagnetic. On theoretical grounds the J_{te} terms are expected to have less weight because the one-electron transfer processes $a_i \leftrightarrow b_j$ are symmetry forbidden.[37]

In $KMg_{1-x}Mn_xF_3$ containing manganese(II) pairs of D_{4h} symmetry, J_{gs} and $J_{eff}'(^4A_1)$ values of 15.0 and 21.2 cm^{-1}, respectively, were determined. Within the present theoretical framework these numbers could be reasonably rationalized only by assuming larger orbital parameters in the excited state.[6]

The absence of any Zeeman splittings of the $^4A_1$ single pair excitations of the bromide complex can be readily explained by the fact that both the ground and excited pair states have g values very close to 2.0. The transitions induced by an exchange-intensity mechanism obey the selection rule $\Delta M_S = 0$. As a consequence, the transitions are not energetically split by a magnetic field despite the substantial splittings of both ground and excited states.

$^4T_2$(D) Singly Excited State. The $^4T_2$(D) single-ion state is split in first order by spin–orbit coupling and a trigonal crystal field component into six Kramers doublets. The order of magnitude of these splittings can be estimated from the energy spread of 31.7 cm^{-1} for bands 9–13 in Figure 7 (bromide) and 41.5 cm^{-1} for bands 7–11 in Figure 9 (chloride). These lines represent pure electronic transitions of isolated manganese(II) centers. Theoretical expectations of these splittings are 1 order of magnitude larger.[30] The observed reduction is most likely the result of a Ham quenching effect. Both spin–orbit coupling and trigonal crystal field matrix elements are susceptible to it.

The orbital degeneracy of $^4T_2$(D) greatly complicates the theoretical treatment of the exchange coupling in manganese pairs. The procedure used for the $^4A_1$ singly excited states is not applicable, since orbital angular momentum must be considered explicitly in a serious theoretical approach. This has not been done so far. There is also the additional complication of the Jahn–Teller effect. This effect is well established, for example, for all ^4T states of manganese(II) in $RbMnF_3$.[38] We therefore restrict ourselves to a more phenomenological discussion of the exchange effects in this singly excited pair state.

Independent of the exact formal treatment of the exchange coupling, it is clear from theoretical considerations that the spin–orbit plus trigonal splitting pattern of the single ion is modified in the dimer and additional splittings are induced. These effects are expected to be of the order of magnitude of J and similar to the combined effects of spin–orbit coupling and trigonal crystal field. Experimentally we find that the total energy spread within the groups of pair bands A and B are similar to, but not identical with, the intervals in the group

(33) Güdel, H. U.; Furrer, A., unpublished results.
(34) Breitling, W.; Lehmann, W.; Weber, R.; Lehner, N.; Wagner, V. *J. Magn. Magn. Mater.* **1977**, *6*, 113.
(35) Eibschütz, M.; Sherwood, R. C.; Hsu, F. S. L.; Cox, D. E. *AIP Conf. Proc.* **1972**, *No. 10*, 684.
(36) Dingle, R.; Lines, M. E.; Holt, S. L. *Phys. Rev.* **1967**, *158*, 489.
(37) Gondaira, K. I.; Tanabe, Y. *J. Phys. Soc. Jpn.* **1966**, *21*, 1527.
(38) Solomon, E. I.; McClure, D. S. *Phys. Rev. B: Solid State* **1974**, *9*, 4690.

9-13 (bromide) and 7-11 (chloride) in support of the above notion.

The fact that the B bands, which correspond to transitions from the $S = 2$ ground level, appear at lower energy than the A bands, which originate in the $S = 1$ level, indicates that J_{eff}' is smaller than J_{gs}. A similar situation was found for the $^4T_1(G)$ state in $KMg_{1-x}Mn_xF_3$.[6] Care is necessary, however, with this interpretation because, strictly speaking, $J_{eff}'(^4T_2)$ is not defined, since an operator of the form (3) does not apply.

Bands 7, 11, and 12 (bromide) deserve special comment. Their decrease in size between 2 and 8 K is compatible only with their assignment as pair transitions originating in the $S = 0$ ground level. (Bands 11 and 12 appear to overlay single-ion absorptions as well.) Since the excited-state spin quantum numbers range from 1 to 4, these bands correspond to $\Delta S = 1$ transitions. Band 7 is 14.5 cm^{-1} higher in energy than band 5, which corresponds to a $\Delta S = 0$ transition originating in the $S = 1$ ground level. Since 14.2 cm^{-1} is the calculated energy of the singlet-triplet separation in the ground state, both transitions 5 and 7 are likely to lead to the same excited level. The occurrence of $\Delta S = 1$ excitations is not surprising when one considers the fact that in this singly excited pair state S is no longer a sharply defined quantum number as a result of spin-orbit coupling.

The observation of Zeeman effects in the $^4T_2(D)$ single pair excitations of the bromide complex can be explained as follows: in contrast to the case of $^4A_1$, the g values in the $^4T_2$ state deviate from 2.0 due to some orbital contributions. This leads to different Zeeman splittings of ground and excited states and thus effective Zeeman splittings even for $\Delta M_S = 0$ as well as $\Delta M_S = \pm 1$ transitions.

$^4E(D)$ Singly Excited State. The region of $^4E(D)$ transitions in the bromide provides a particularly fine example of a pair spectrum. The bands 1 and 2 (Figure 10) have the same temperature dependence as the A bands in the $^4A_1$ and $^4T_2$ regions. From this we can assign them to transitions originating in the $S = 1$ ground level. The energy difference between bands 1 and 2 corresponds to an excited-state splitting. It is most likely a result of the combined effects of spin-orbit coupling and trigonal crystal field, which are expected to produce a second-order splitting of the order of a few wave numbers.[4] Bands 3 and 4 are identified from their temperature dependence as cold pair bands originating in the $S = 0$ pair level. They are displaced from bands 1 and 2 by 14.0 cm^{-1}, the singlet-triplet separation of the ground state. The corresponding energy level diagram including the observed transitions is shown in Figure 10. Bands 5 and 6 are probably single-ion transitions to two spin-orbit components of ^4E.

We have not observed any $2 \rightarrow 2$ pair transition for this state. At the highest temperature used (ca. 20 K) the corresponding bands are expected to be still rather weak. And if they lie at higher energy than the $1 \rightarrow 1$ bands, as was the case for $KMg_{1-x}Mn_xF_3$,[6] they could lie beneath the other more intense bands observed in this region.

The chloride spectrum is much less resolved in this region. Between 19.8 and 1.4 K a band at 27 794 cm^{-1} decreases sharply in size and vanishes at 1.4 K. We therefore assign it to a pair transition originating in the $S = 1$ level. A weak band lying 21 cm^{-1} higher in energy is assigned to a pair transition originating in the $S = 0$ level. This energy difference (21 cm^{-1}) is in good agreement with a J_{gs} value of 19.6 cm^{-1} determined from the temperature dependence of the $^4A_1$ pair excitations. A third peak lies at 27 837 cm^{-1}, and it is relatively insensitive to temperature in the range studied. It probably represents a single-ion transition.

We have then, through the use of high-resolution absorption and Zeeman spectroscopy, identified manganese(II) pair excitations in $CsMg_{1-x}Mn_xX_3$ (X = Br, Cl) to the singly excited $^4A_1(G)$, $^4T_2(D)$, and $^4E(D)$ states. A full analysis has been carried out only for the $^4A_1$ pair transitions. For the other two orbitally degenerate, singly excited states a simple theoretical model is not yet available.

Acknowledgment. We thank the Swiss National Science Foundation for support (Grant No. 2.427-0.79) and Naomi Furer for preparing the crystals used in this study.

Registry No. $CsMnBr_3$, 36482-50-5; $Mn_2Br_9^{5-}$, 88780-80-7; $Mn_2Cl_9^{5-}$, 58396-13-7.

Contribution from the Department of Chemistry, McMaster University, Hamilton, Ontario L8S 4M1, Canada

^{199}Hg NMR Study of the Hg^{2+}, Hg_2^{2+}, Hg_3^{2+}, and Hg_4^{2+} Cations: The First Example of Hg-Hg Spin-Spin Coupling

RONALD J. GILLESPIE, PIERRE GRANGER,[1] KEITH R. MORGAN, and GARY J. SCHROBILGEN*

Received June 7, 1983

The mercury cations Hg^{2+}, Hg_2^{2+}, Hg_3^{2+}, and Hg_4^{2+} have been studied by ^{199}Hg NMR spectroscopy. For Hg^{2+} and Hg_2^{2+} well-resolved resonances were observed over a wide range of temperatures. For Hg_3^{2+}, only at temperatures less than -40 °C were resonances sufficiently sharp to be observed, and at no temperature down to -70 °C were sharp ^{199}Hg resonances observed in solutions of Hg_4^{2+}. The ^{199}Hg NMR spectra of Hg_3^{2+} show second-order effects due to coupled mercury atoms, and a value for $J_{^{199}Hg-^{199}Hg}$ of 139 600 Hz was obtained, representing the first Hg-Hg and largest nuclear spin-spin coupling constant reported to date.

Introduction

The homopolyatomic cations of mercury can be prepared by oxidation of elemental mercury with a pentafluoride, MF_5 (M = As or Sb), or with Hg^{2+} cation in a suitably weakly basic solvent medium such as SO_2 to give successively Hg_2^{2+}, Hg_3^{2+}, Hg_4^{2+},[2,3] and the linear-chain metallic compounds $Hg_{3-\delta}MF_6$.[4,5] The resulting SO_2-soluble cations Hg_2^{2+}, Hg_3^{2+}, and Hg_4^{2+} and the insoluble linear-chain metallic compounds $Hg_{2.85}AsF_6$ and $Hg_{2.91}SbF_6$ have all been characterized in the solid state

(1) Present address: Département de Chimie, IUT de Rouen, 76130 Mont-Saint-Aignan, France.

(2) Davies, C. G.; Dean, P. A. W.; Gillespie, R. J.; Ummat, P. K. *J. Chem. Soc. D* **1971**, 782.
(3) Cutforth, B. D.; Gillespie, R. J.; Ireland, P. R. *J. Chem. Soc., Chem. Commun.* **1973**, 723.
(4) Cutforth, B. D.; Davies, C. G.; Dean, P. A. W.; Gillespie, R. J.; Ireland, P. R.; Ummat, P. K. *Inorg. Chem.* **1979**, *12*, 1343.
(5) Gillespie, R. J.; Ummat, P. K. *J. Chem. Soc. D* **1971**, 1168.

0020-1669/84/1323-0887$01.50/0